Int J Fract (2008) 154:51–59
DOI 10.1007/s10704-008-9306-3

ORIGINAL PAPER

Fracture size effects from disordered lattice models

Mikko J. Alava · Phani K. V. V. Nukala · Stefano Zapperi

Received: 14 April 2008 / Accepted: 17 December 2008

Abstract We study size effects in the fracture strength of notched quasi-brittle materials using numerical simulations of lattice models for fracture. In particular, we consider the random fuse model, the random spring model and the random beam model, which all give similar results. These allow us to establish and understand the crossover between a regime controlled by disorder-induced statistical effects and a stress-concentration controlled regime ruled by fracture mechanics. The crossover is described by a scaling law that accounts for the presence of fracture process zone which we quantify by averaging over several disordered configurations of the model. The models can be used to study the development of the fracture process zone as the load is increased and to express this in terms of crack resistance (R-curve).

M. J. Alava
Department of Applied Physics, Helsinki University of Technology (HUT), Helsinki 02015, Finland

P. K. V. V. Nukala
Computer Science and Mathematics Division, Oak Ridge National Laboratory, Oak Ridge, TN 37831-6164, USA

S. Zapperi (✉)
CNR-INFM, S3, Dipartimento di Fisica, Università di Modena e Reggio Emilia, Via G. Campi 213A, Modena, Italy
e-mail: stefano.zapperi@unimore.it

S. Zapperi
ISI Foundation, Viale S. Severo 65, 10133 Torino, Italy

Keywords Fracture · Size effect · Notch · Statistical models · Disorder

1 Introduction

Predicting the fracture strength of materials is difficult due to its non-trivial dependence on the characteristic lengthscales of the samples. Size effects are rooted in the structural disorder present in the material: the strength is dominated by the weakest part (subvolume) of the sample and its distribution can in principle be computed using extreme value statistics (Gumbel 2004). The quantitative understanding of this statistical size effect is difficult, since the important low-strength tails of the strength probability distribution are not easy to sample and since the material properties are often history-dependent. For instance, in quasi-brittle materials such as concrete and many other composites, sample failure is preceded by significant damage accumulation (van Mier 1996).

An important engineering scenario and a typical experimental setting is to study the size effect in the presence of a pre-existing flaw, *a notch*. Failure in this case is determined by the competition between deterministic effects, due to the stress enhancement created by notch, and the response of the disordered material to the stress concentration around the defect (Bazant and Planas 1997; Bazant 1999). This includes the stochastic damage accumulation. The effect of disorder can be treated in an effective medium sense by defining a Fracture Process Zone (FPZ) around the crack tip.

For quasi-brittle materials, the size of this FPZ may not be negligible compared to the system size. Conversely, for small notches, failure is more influenced by the FPZ than the notch itself, and depends on statistical disorder effects. Experimentally, it has been demonstrated that the critical crack may nucleate and propagate far from the pre-existing notch (Rosti et al. 2001) in that case.

The existing theories on the size effect start from linear elastic fracture mechanics (LEFM). Several formulations have been proposed in the literature and partly compared with experiments (Bazant 1999; Hu and Wittmann 1992; Karihaloo 1999; Bazant 2000, 2004; Morel et al. 2000, 2002). In the size-effect law proposed by Bazant for quasi-brittle materials (Bazant 1999, Bazant 2000, 2004), the strength of a notched sample is obtained from energy considerations involving a lengthscale ξ due to the presence of a FPZ

$$\sigma_c = \frac{K_c}{\sqrt{\xi + a_0}}, \qquad (1)$$

where a_0 is the linear size of the notch and the critical stress intensity factor $K_c \sim \sqrt{EG_c}$ is a function of the fracture toughness G_c and the elastic modulus E (Griffith 1920).

Equation 1 takes into account both the limits of a very large notch compared to the FPZ size and that of a very small notch. In the limit $a_0 \gg \xi$ one has an expression that follows the LEFM scaling, $\sigma_c \sim 1/\sqrt{a_0}$. In the opposite limit of $a_0 \ll \xi$, the average strength is taken to be constant. Equation 1 has been shown to be in agreement with several experimental data sets (Bazant 2004). However, three fundamental questions can be asked: first, does Eq. 1 incorporate all the important effects? Second, what is the fracture toughness G_c in the presence of disorder? Third, where does the FPZ scale ξ originate and how does it depend again on the disorder?

In this work we clarify the role of the disorder in the failure of notched quasi-brittle specimens using extensive simulations of disordered lattice models for fracture (Alava et al. 2006). A brief account of the results for the random fuse model (RFM) has been published in Alava et al. (2008). In more detail, we consider the RFM, the random spring model (RSM) and the random beam model (RBM). We consider the failure of notched disordered samples and provide a microscopic justification of Eq. 1. Studying the size scaling of strength by extensive numerical simulations is a difficult task due to the different length scales involved and the need of significant statistical averaging. We vary the disorder, which we model as a locally varying random failure threshold, and show that it plays a crucial role in determining the size effect. In particular, a lengthscale ξ emerges from the simulations and can be shown to be directly related to the FPZ size. Finally, for notch sizes smaller than a critical length a_c, we observe a cross-over to the inherent, sample-size dependent strength of the unnotched sample. In order to describe this cross-over, Eq. 1 should be modified as

$$\sigma_c = \frac{K_c}{\sqrt{\xi + a_0 f(a_c(L)/a_0)}}, \qquad (2)$$

where $a_c(L)$ is a system-size dependent cross-over lengthscale and $f(x)$ is an appropriate cross-over function. Equations 1 and 2 are the same in the limit of a_0 large, while in the opposite case the argument of the square root becomes a_c, so that the strength acquires an explicit dependence on L as we discuss below. We show that the RFM results are confirmed in the RSM and the RBM. We also study the growth of the FPZ, showing that it is independent of the notch size a_0 and the system size L.

2 Models

2.1 Random fuse model

The RFM (de Arcangelis et al. 1985) provides a scalar electrical analogy of elasticity, formally corresponding to an antiplanar shear deformation. In the RFM, we consider a triangular lattice of conductive bonds. At each node i, the voltage V_i satisfies the Kirchhoff equation with appropriate boundary conditions

$$\sum_j \sigma_{ij}(V_i - V_j) = 0, \qquad (3)$$

where σ_{ij} is the local conductivity of the fuse connecting nodes i and j. The currents in each bond are then obtained from the Ohm law. Initially each fuse has the same conductance and a random breaking threshold t. This represents a locally varying fracture toughness/strength. The t lie between 0 and 1, with a cumulative distribution $P(t) = t^{1/D}$, where D represents a quantitative measure of disorder. The larger D is, the stronger the disorder. The characteristics of a fuse is such that burning of a fuse occurs irreversibly, whenever the electrical current in the fuse exceeds breaking threshold t of the fuse; however, in our simulations, the dynamics is controlled by burning the most critical fuse during each step. Periodic boundary conditions are imposed in the horizontal direction to simulate an infinite system and a constant voltage difference, V, is applied between the top and the bottom of lattice system bus bars. Numerically, a unit voltage difference, $V = 1$, is set between the bus bars and the Kirchhoff equations are solved to determine the current flowing in each of the fuses. Subsequently, for each fuse j, the ratio between the current i_j and the breaking threshold t_j is evaluated, and the bond j_c having the largest value, $\max_j \frac{i_j}{t_j}$, is irreversibly removed (burnt). The current is redistributed instantaneously after a fuse is burnt implying that the current relaxation in the lattice system is much faster than the breaking of a fuse. Each time a fuse is burnt, it is necessary to re-calculate the current redistribution in the lattice to determine the subsequent breaking of a bond. The process of breaking of a bond, one at a time, is repeated until the lattice system fails completely. In the present simulations, we have considered horizontal notches (see Fig. 1) with various sizes for lattices of size $L = 64, 128, 192, 256, 320$ and disorder $D = 0.1, 0.3, 0.5, 0.6, 0.75$.

2.2 Random spring model

The RSM (Sahimi and Goddard 1986; Hansen et al. 1989; Arbabi and Sahimi 1993; Sahimi and Arbabi 1993; Nukala et al. 2005) is based on a triangular lattice with nodes connected by linear springs, defined by the Hamiltonian

$$H = \sum_{ij} \frac{K}{2} (\mathbf{u}_i - \mathbf{u}_j)^2 \tag{4}$$

where $\mathbf{u}_i$ is the displacement of node i and K is the spring constant, which we set to unity. The elastic equilibrium is obtained by minimizing Eq. 4. Despite the fact that the RSM suffers from the caveats associated with the presence of soft modes, it is still considered quite often in the context of fracture. In terms of continuum elasticity, the discrete triangular central-force lattice model represents an isotropic elastic medium with a fixed Poisson's ratio of $1/3$ in two-dimensions, and $1/4$ in three-dimensions. As for the RFM, the bond breaking thresholds, t, are randomly distributed based on a thresholds cumulative probability distribution, $P(t) = t^{1/D}$ for $t \in [0, 1]$. The constitutive law of springs is linear elastic and perfectly brittle such that the spring breaks irreversibly, whenever the force in the spring

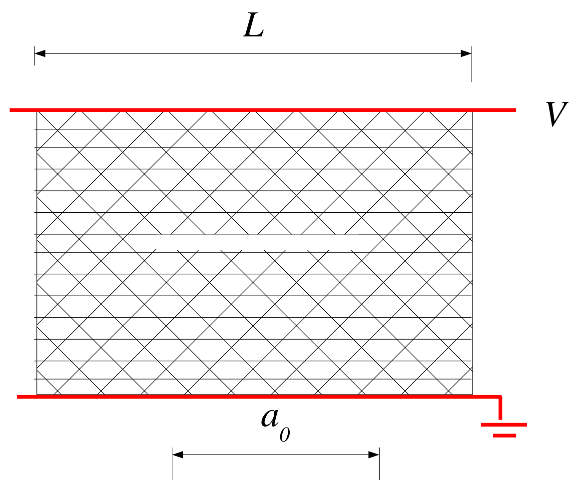

Fig. 1 The geometry employed for the simulations of the RFM. An horizontal notch of length a_0 is introduced at the center of a triangular lattice of linear size L. A voltage drop is applied over the vertical direction. The geometry for the RSM and the RBM is similar, with a displacement applied in the vertical direction

exceeds the breaking threshold force value, t, of the spring. However, the dynamics of the simulaion proceeds by breaking the most critical spring during each step. Periodic boundary conditions are imposed in the horizontal direction and a displacement difference is applied between the top and the bottom of the lattice system. Numerically, a unit displacement, $\Delta = 1$, is applied at the top of the lattice system and the equilibrium equations are solved to determine the force in each of the springs. Subsequently, for each bond j, the ratio between the force f_j and the breaking threshold t_j is evaluated, and the bond j_c having the largest value, $\max_j \frac{f_j}{t_j}$, is irreversibly removed. The forces are redistributed instantaneously after a bond is broken implying that the stress relaxation in the lattice system is much faster than the breaking of a bond. Each time a bond is broken, it is necessary to re-equilibrate the lattice system in order to determine the subsequent breaking of a bond. The process of breaking of a bond, one at a time, is repeated until the lattice system falls apart. For the RSM, we consider a triangular lattice network of size L with a notch of size a_0 in the horizontal direction. In the present simulations, we have considered various notch sizes for $L = 128, 256$ and $D = 0.5, 0.6$.

2.3 Random beam model

In the random thresholds beam model (RBM) (Roux and Guyon 1985; Herrmann et al. 1989), we consider a two-dimensional triangle lattice system of linear size L. The RBM has three degrees of freedom (x-translation u, y-translation v, and a rotation θ about z axis) at each of the lattice nodes (sites), and each of the bonds (beams) in the lattice connects two nearest neighbor nodes. We assume that the beams are connected rigidly at each of the nodes such that the angle between any two beams connected at a node remains unaltered during the deformation process. These nodal displacements and rotations introduce conjugate forces and bending moments in the beam members, described by Timoshenko beam theory (Przemieniecki 1968) which includes shear deformations of the beam cross-section in addition to the usual axial deformation of cross-sections. In the present simulation, we start with a notched lattice system with beams having unit length, unit square cross-section and Young's modulus $E = 1$. This results in a unit axial stiffness ($EA/\ell_b = 1$) and bending stiffness ($12EI_0/\ell_b^3 = 1$) for each of the beams in the lattice system. Here, A is the beam cross-sectional area, I is the moment of inertia of beam cross-section and ℓ_b is the length of the beam. Since the beam can deform in two independent deformation modes (axial and bending), we assume randomly distributed bond breaking axial and bending thresholds, t_a and t_b, based on thresholds cumulative probability distributions, $P_a(t_a)$ and $P_b(t_b)$ respectively. As in the other models, the cumulative distributions are defined as $P(t) = t^{1/D}$ in [0, 1].

The failure criterion for a beam is defined through an axial force F and bending moment M interaction equation given by

$$r \equiv \left(\frac{F}{t_a}\right)^2 + \frac{\max(|M_i|, |M_j|)}{t_b} = 1 \tag{5}$$

The beam breaks irreversibly, whenever the failure criterion $r \geq 1$. Notice once again that $r \geq 1$ merely represents a failure criterion for the beams. The dynamics of the simulations however are characterized by breaking the most critical beam during each step. Periodic boundary conditions are imposed in the horizontal direction and a constant unit displacement difference is applied between the top and the bottom of lattice system.

Numerically, a unit displacement, $\Delta = 1$, is applied at the top of the lattice system and the equilibrium equations for forces and torques are solved to determine the displacements of each of the beams. The forces are redistributed instantaneously after a bond is broken implying as in the other models that the stress relaxation in the lattice system is much faster than the breaking of a bond. Each time a bond is broken, it is necessary to re-equilibrate the lattice system in order to determine the subsequent breaking of a bond. The process of breaking of a bond, one at a time, is repeated until the lattice system falls apart.

3 Strength and size effects

We perform numerical simulations of the models discussed above, concentrating on the failure strength. Notice that the three models differ mainly in the way stress is redistributed. To illustrate this point, we report in Fig. 2 the stress concentration profiles in a triangular lattice ($L = 512$) with a notch of size $a_0 = 16$. Although the angular distribution of the stress profiles differs, the way stress decays from the crack tip is very similar, approaching for large L the $1/\sqrt{x}$ decay, where x is the distance from the crack tip, expected from the theory of elasticity.

In order to obtain reliable results, the strength should be averaged over several realizations of the disorder. In the present simulations, we have used a minimum of $N_r = 200$ realizations and in some cases up to $N_r = 8000$ realizations. Figure 3a reports the strength σ_c, averaged over different configurations, with varying a_0 and D for the RFM. The most instructive way of

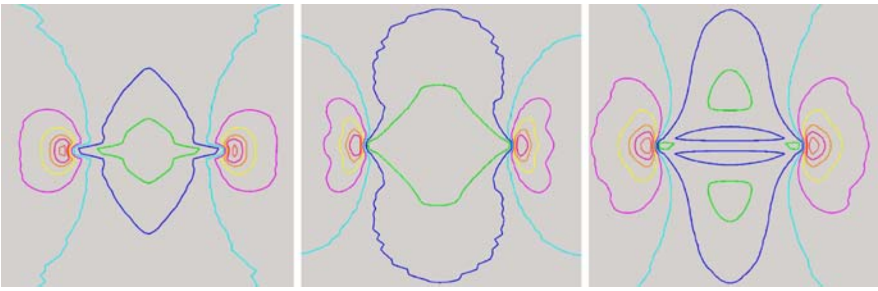

Fig. 2 The stress concentration profiles for the RFM (left), the RSM (center) and the RBM (right)

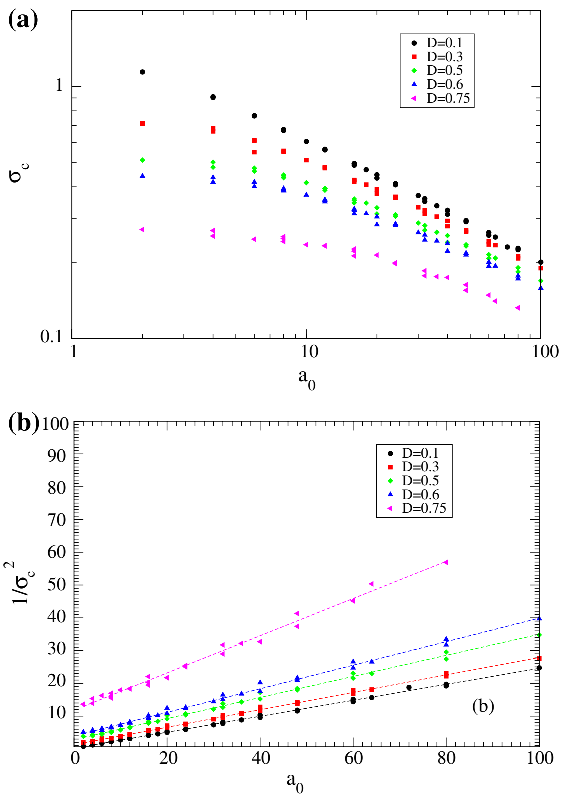

Fig. 3 **a** The strength in the RFM for several disorders D and notch sizes a_0. **b** A scaling plot of the data according to Eq. 1

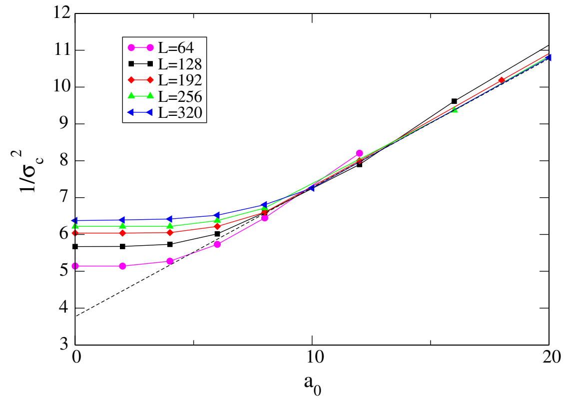

Fig. 4 A close-up of the strength data of the RFM for $D = 0.6$, showing the dependence on the system size L for small a_0

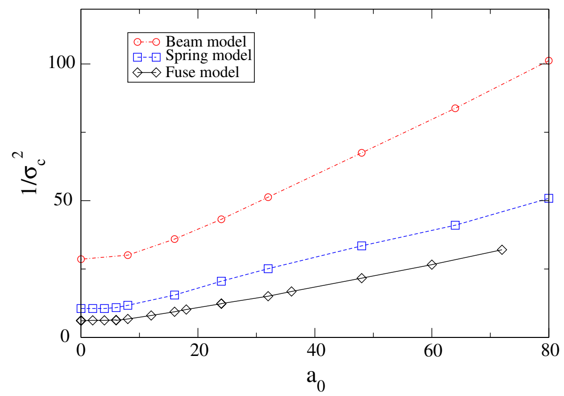

Fig. 5 A scaling plot of the strength according to Eq. 1 for the RFM (for $L = 192$, $D = 0.6$), the RSM ($L = 256$ $D = 0.5$) and the RBM ($L = 256$ $D = 1.0$) models. The qualitative features of the data for different system sizes and disorders are the same in all the three models

plotting is to consider the inverted square strength, $1/\sigma_c^2$. Assuming Eq. 1, $1/\sigma_c^2$ should become a linear function of a_0 for large enough notches. Plotting the data in this way in Fig. 3b shows that for $a_0 \gg 1$, the scaling of Eq. 1 is recovered asymptotically. Extrapolating the linear part towards $a_0 = 0$, we can define a disorder-dependent intercept $\xi(D)$, that should be related to the FPZ size. Furthermore, the slope of the linear part of the data ($1/K_c^2(D)$) is also disorder-dependent, which implies a disorder-dependent fracture toughness $G_c(D)$. Finally, a careful observation reveals that for small a_0 less than a critical crack size a_c, the strength scaling crosses over from a stress concentration dominated LEFM scaling (Eq. 1) to a disorder dominated scaling (see Fig. 4). That is, for $a_0 \ll a_c$, the strength scaling deviates significantly from Eq. 1 and saturates to a value that depends on disorder and the sample size, $\sigma_c(L, D)$. In particular, the strength of the unnotched system (for $a_0 = 0$) is finite and is smaller than the LEFM limit $K_c/\sqrt{\xi}$ given by Eq. 1. In Fig. 5, we present a comparison between RFM, RSM and the RBM. The general features of the strength are the same in the three models, indicating that only the decay of stress concentration is relevant for the size effect, while the precise angular dependence of stress concentration around a notch is not important.

In Alava et al. (2008) we presented a scaling theory that extends the earlier scaling law given by Eq. 1 beyond its actual regime of validity. A correct scaling expression has to accommodate the three separate phenomena visibile in Figs. 3–4: for small notches, the dominance of statistical effects that dictate $\sigma_c(L, D)$, the cross-over to the LEFM-like regime, and then finally an Eq. 1 like scaling at large a_0.

The cross-over takes place at a scale a_c above which σ_c follows Eq. 1. For small notches, $a_0 \ll a_c$ the strength is determined by extremal statistics as is appropriate in the limit $a_0 \to 0$ (Alava et al. 2006). Then one expects to see a weak size effect, typically logarithmic in L. In real materials, the scaling will depend on the damage accumulation and the defect populations that exist in the specimens. $\sigma_c(L, D)$ is not a constant however, as Eq. 1 would predict, and deviates significantly from the LEFM-based theory, which would in general predict that the samples are weaker than their actual strength $\sigma_c(L, D)$.

The location of the cross-over (notch size) a_c follows by equating the strength prediction of Eq. 1 and the scaling of notchless specimes, $1/\sigma(L, D)^2 \simeq (a_c + \xi)/K_c^2$. An appropriate scaling theory, valid for all a_0, is then

$$\frac{K_c^2}{\sigma_c^2} = \xi + a_0 f(a_c/a_0) \tag{6}$$

where the scaling function $f(y)$ has the limits

$$f(y) \simeq \begin{cases} 1 \text{ if } & y \ll 1 \\ y \text{ if } & y \gg 1 \end{cases} \tag{7}$$

Thus we have for the cross-over scale

$$a_c \simeq (K_c(D)/\sigma_c(L, D))^2 - \xi(D). \tag{8}$$

For $a_0 > a_c$, fracture is governed by LEFM and a scaling of the kind of Eq. 1 is recovered. The effect of disorder, according to the scaling theory, is incorporated in the three parameters $\sigma_c(L, D)$, $K_c(D)$, and $\xi(D)$. In the following, we first discuss the first two parameters and return to ξ below in much more detail. Qualitatively (since the behaviour of $\sigma_c(L, D)$ is an independent issue entirely), the effect of changing disorder strength for a fixed L can be seen as follows. For stronger disorder, the cross-over will take place at larger a_c, since the stress concentration of the notch will be blunted (as we demonstrate below). At fixed disorder, a_c increases with L since notchless specimens get weaker. The fracture toughness G_c (since in the models $E = 1$) seems in our simulations to be proportional to the average model element strength at weak disorder at least, and perhaps gets reduced with strong disorder (Alava et al. 2008). More numerical work in this direction might be interesting.

4 The fracture process zone

Our numerical simulations allow to monitor the damage evolution prior to failure and can thus be used to study the development of the FPZ. For a single realization of the disorder, we only see diffuse damage up to the peak load, and it is difficult to determine the size of the FPZ. On the other hand, the FPZ can be clearly measured after averaging the damage over several realizations of the disorder. Hence, the size of FPZ should thus be considered in statistical terms as the region around the crack tip where damage is most likely to occur. Considering for simplification a projection of the average damage along the notch main axis direction, we obtain a profile that is decaying exponentially towards a homogeneous background value (see Fig. 6):

$$d(x) = A + B \exp{(-2x/\xi_{FPZ})}. \tag{9}$$

The factor 2 in the exponential comes from the fact that in our geometry the FPZ extends from the two edges of the notch. We have analyzed the data for different values of a_0 and L in order to check that the profiles do not

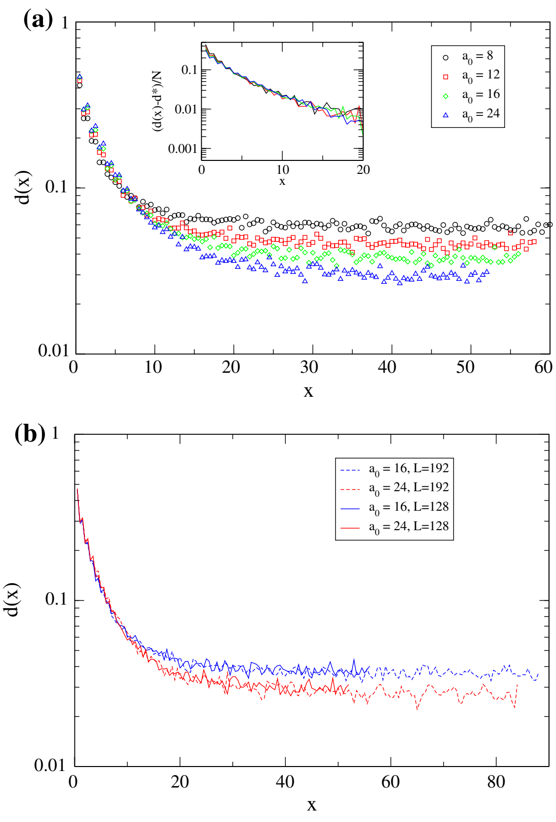

Fig. 6 **a** Damage profiles along the crack axis for various notch sizes a_0. Damage profiles follow an exponential decay on a uniform damage background. In order to show that ξ_{FPZ} is independent on a_0, we report in the inset the profiles after subtracting the background and normalizing so that the curves superimpose. **b** Damage profiles for two different lattice sizes L and two different notch sizes a_0. The profiles do not depend on L

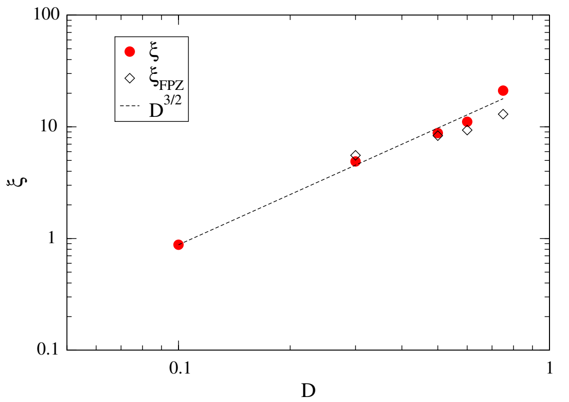

Fig. 7 The dependence of the FPZ size on disorder for the RFM ($L = 128$, $a_0 = 16$). Estimates from the strength (ξ from Eq. 1) and from damage profiles (ξ_{FPZ} from Eq. 9) are similar. We could not obtain reliable estimates from damage profiles for very weak disorder ($D = 0.1$)

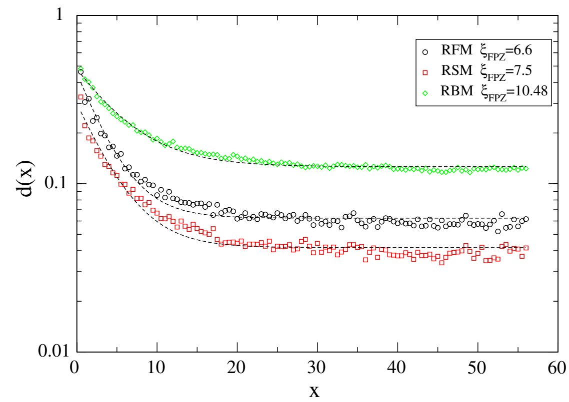

Fig. 8 A comparison of the damage profiles measured in RFM, RSM and RBM using system size $L = 128$, disorder $D = 0.6$, and an initial notch size $a_0 = 16$. Two thousand samples are used for averaging the damage profiles. The result show that while the profiles are qualitatively similar ξ_{FPZ} and the damage backgo-und differ

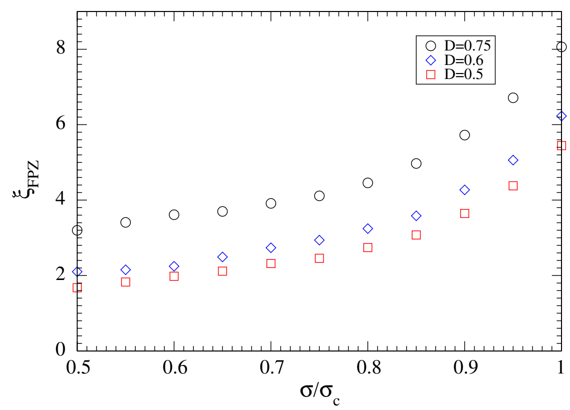

Fig. 9 The FPZ size as a function of the applied stress normalized by the peak stress as obtained from damage profiles (Eq. 9). Data are for RFM for different values of disorder ($a_0 = 16$, $L = 128$)

depend on L and on a_0, as long as this is not too far from a_c. For $a_0 \ll a_c$ we naturally do not expect to see such a "damage cloud" around the original defect. However, it seems likely that one could measure ξ around the most critical microcrack. Recall that in this regime one expects the strength to saturate at $\sigma_c = \sqrt{K_c/(a_c + \xi)}$.

Notice that the LEFM stress intensity factor would indicate a $1/\sqrt{x}$-like divergence of the stress at the crack tip. It is evident that the observed exponential decay of damage profile d is in contrast to a $1/\sqrt{x}$-like decay and should be naturally interpreted as a screening of the crack tip caused by the disorder. In fact, the FPZ size ξ_{FPZ} depends on the disorder strength D as shown in Fig. 7. The data can be roughly described by a power law relation $\xi_{FPZ} \sim D^{3/2}$. As discussed in (Alava et al. 2008), if we plot the fracture process size $\xi_{FPZ}(D)$ against the intrinsic scale ξ resulting from the fits of the strength data to Eq. 1, we obtain a linear relation. Hence, we can conclude that ξ is indeed a direct measure of the FPZ size. Figure 8 reports a comparison of the damage profiles in RFM, RSM and RBM. It can be seen that the results are qualitatively similar for all the three models considered. The value of the FPZ size ξ_{FPZ}, however, differs slightly for the three models.

The FPZ progressively develops before the peak load by damage accumulation. To visualize this process, we have computed damage profiles at different values of the applied stress. One can then obtain the FPZ size $\xi_{FPZ}(D)$ as a function of the stress. As can be seen in Fig. 9, there is a gradual increase of $\xi_{FPZ}(D)$ with stress. This growth relates to the R-curve of the material (Morel et al. 2000) which is usually defined in terms of the elastic energy released due to crack growth $G \equiv \partial U/\partial a$ (Bazant and Planas 1997). In the RFM model, we can derive G from the lattice "elastic" energy $U = I^2/(2\Sigma)$, where Σ is the conductivity, as

$$G \approx \frac{\Delta U}{\Delta a} = \frac{I^2}{2\Sigma^2}\frac{\Delta\Sigma}{\Delta a} \tag{10}$$

where $\Delta\Sigma = (\Sigma_0 - \Sigma)$ is the conductivity change after the crack has extended by Δa such that $a = a_0 + \Delta a$, and Σ_0 is the initial conductivity. We report the R-curve for different values of disorder in Fig. 10. The data is

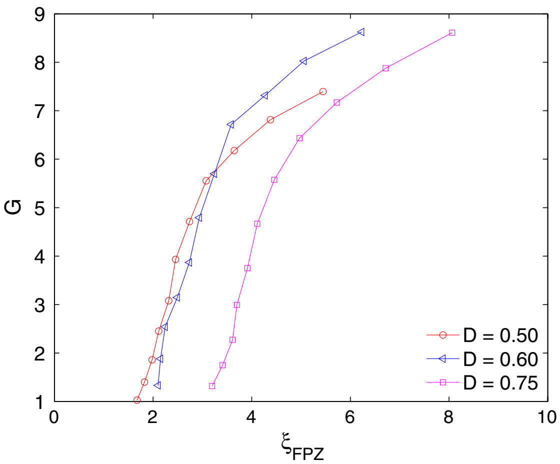

Fig. 10 The R curve of the RFM for different values of the disorder D. G is obtained from Eq. 10 and ξ_{FPZ} is obtained from Eq. 9

shown for the current values $I \in [I_c/2, I_c]$ in which $\xi(I)$ can be extracted from the damage profiles with a reliable accuracy. In this regime the R-curves show in general two behaviors: an initial rapid increase due to the accumulating damage that changes the average conductivity, followed by a saturation as the FPZ starts to increase even more rapidly. The conductivity change is a mean-field phenomenon that accounts for the total damage in the system and thus to the failure thresholds $P(i_c)$. The growth of $\xi(I)$ is not expected to be so simply related to the damage. It is interesting to note that as a result the R-curves for various disorders overlap in the manner depicted in Fig. 10. The size-dependence of these R-curves would be expected to be negligible as long as the strength is governed by Eq. 1.

5 Conclusion

We have resorted to simulations of statistical fracture models to analyze the problem of the size-effect in the failure of quasi-brittle materials. For large notches, the simulations recover the expression based on LEFM (Bazant 1999, 2000, 2004) and allow to relate the effective FPZ size ξ to the actual average damage profiles. As the notch size is decreased we observe a crossover at a novel scale a_c to a disorder-dominated size-dependent regime that is not described by LEFM and is furthermore seen in experiments (Alava et al. 2008). All the regimes are summarized in a generalized scaling expression for the strength of disordered media.

Several interesting future questions remain, like theoretical computations of parameters such as a_c, K_c, and the detailed understanding of the origin and shape of the statistical FPZ. These would be in particular important in order to help to achieve practical predictions. Recall our results have shown, that all such parameters are dependent on disorder, which in the models used translates into the damage accumulated at a given local stress. This quantity is evidently hard to access experimentally, but is unfortunately theoretically necessary. For such reasons, it would be relevant to investigate three dimensional systems and possibly look at other kinds of disorder (eg. locally varying elastic moduli).

Acknowledgments MJA would like to acknowledge the support of the Center of Excellence-program of the Academy of Finland. MJA and SZ gratefully thank the financial support of the European Commissions NEST Pathfinder programme TRIGS under contract NEST-2005-PATH-COM-043386. PKKVN acknowledges support from Mathematical, Information and Computational Sciences Division, Office of Advanced Scientific Computing Research, U.S. Department of Energy under contract number DE-AC05-00OR22725 with UT-Battelle, LLC. PKKVN also acknowledges the use of IBM BG/L resources made available to him at Argonne National Laboratory through INCITE.

References

Alava MJ, Nukala P, Zapperi S (2006) Statistical models for fracture. Adv Phys 55:349–476
Alava MJ, Nukala P, Zapperi S (2008) Role of disorder in the size scaling of material strength. Phys Rev Lett 100:055502
Arbabi S, Sahimi M (1993) Mechanics of disordered solids I. Percolation on elastic networks with central forces. Phys Rev B 47(2):695–702
Bazant ZP (1999) Size effect on structural strength: a review. Arch Appl Mech 69:703–725
Bazant ZP (2000) Size effects. Int J Solids Struct 37:69–80
Bazant ZP (2004) Scaling theory for quasi brittle structural failure. PNAS 101:13400–13407
Bazant ZP, Planas J (1997) Fracture and size effect in concrete and other quasibrittle materials. CRC Press, Boca Raton
de Arcangelis L, Redner S, Herrmann HJ (1985) A random fuse model for breaking processes. J Phys (Paris) Lett 46(13):585–590
Gumbel EJ (2004) Statistics of extremes. Columbia University Press, New York
Griffith AA (1920) The phenomenon of rupture and flow in solids. Trans R Soc (London) A 221:163–198
Hansen A, Roux S, Herrmann HJ (1989) Fracture of disordered, elastic lattices in two dimensions. J Phys 50:733–744

Herrmann HJ, Hansen A, Roux S (1989) Fracture of disordered, elastic lattices in two dimensions. Phys Rev B 39(1):637–648

Hu XZ, Wittmann F (1992) Fracture energy and fracture process zone. Mat Struct 25:319–326

Karihaloo B (1999) Size effect in shallow and deep notched quasi-brittle structures. Int J Fract 95:379–390

Morel S, Schmittbuhl J, Bouchaud E, Valentin G (2000) Scaling of crack surfaces and implications on fracture mechanics. Phys Rev Lett 85:1678–1681

Morel S, Bouchaud E, Valentin G (2002) Size effects in fracture: roughening of crack surfaces and asymptotic analysis. Phys Rev B 65:104101

Nukala PKVV, Zapperi S, Simunovic S (2005) Crack roughness and avalanche precursors in the random fuse model. Phys Rev E 71:066106

Przemieniecki JS (1968) Theory of matrix structural analysis. McGraw-Hill Book Company, New York

Rosti J, Salminen LI, Seppälä ET, Alava MJ, Niskanen KJ (2001) Pinning of cracks in two-dimensional disordered media. Eur Phys J B 19:259–263

Roux S, Guyon E (1985) Mechanical percolation: a small beam lattice study. J Phys Lett 46:L999–1004

Sahimi M, Arbabi S (1993) Mechanics of disordered solids. II. Percolation on elastic networks with bond-bending forces. Phys Rev B 47:703–712

Sahimi M, Goddard JD (1986) Elastic percolation models for cohesive mechanical. Failure in heterogeneous systems. Phys Rev B 33:7848–7851

van Mier JGM (1996) Fracture processes of concrete. CRC Press, Boca Raton